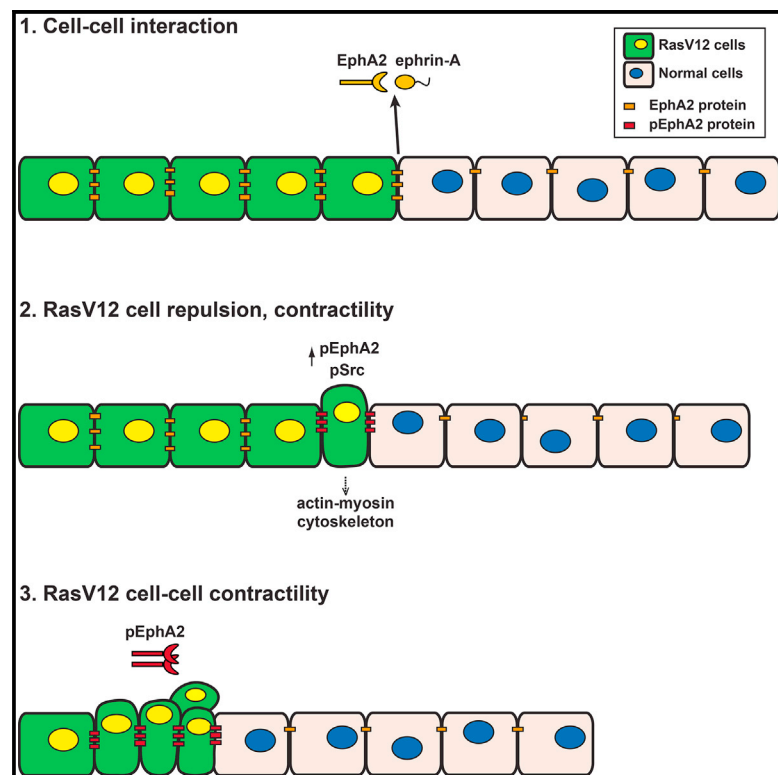


# Current Biology

## EphA2 Drives the Segregation of Ras-Transformed Epithelial Cells from Normal Neighbors

### Graphical Abstract



### Authors

Sean Porazinski,  
Joaquín de Navascués, Yuta Yako, ...,  
Robert Maddison, Yasuyuki Fujita,  
Catherine Hogan

### Correspondence

hoganc@cardiff.ac.uk

### In Brief

Porazinski et al. demonstrate that differential Eph receptor signaling is required for the detection of Ras-transformed epithelial cells within epithelial sheets in vitro and in vivo. Cell-cell interactions with normal neighbors trigger Eph-dependent signals, which drive RasV12 cell segregation from normal cells at the single and multicellular levels.

### Highlights

- Normal epithelial cells detect Ras-transformed neighbors expressing elevated EphA2
- Cell-cell interaction between normal and RasV12 cells induces ephrin-A-EphA2 signals
- Differential EphA2 signaling drives RasV12 cell repulsion and contractility
- *Drosophila* Eph is required to drive segregation of RasV12 cells in vivo



# EphA2 Drives the Segregation of Ras-Transformed Epithelial Cells from Normal Neighbors

Sean Porazinski,<sup>1</sup> Joaquín de Navascués,<sup>1</sup> Yuta Yako,<sup>2</sup> William Hill,<sup>1</sup> Matthew Robert Jones,<sup>1</sup> Robert Maddison,<sup>1</sup> Yasuyuki Fujita,<sup>2</sup> and Catherine Hogan<sup>1,3,\*</sup>

<sup>1</sup>European Cancer Stem Cell Research Institute, Cardiff University, Hadyn Ellis Building, Maindy Road, Cardiff CF24 4HQ, UK

<sup>2</sup>Division of Molecular Oncology, Institute for Genetic Medicine, Hokkaido University Graduate School of Chemical Sciences and Engineering, Kita 15, Nishi 7, Kita-ku, Sapporo, Hokkaido 060-0815, Japan

<sup>3</sup>Lead Contact

\*Correspondence: [hoganc@cardiff.ac.uk](mailto:hoganc@cardiff.ac.uk)

<http://dx.doi.org/10.1016/j.cub.2016.09.037>

## SUMMARY

In epithelial tissues, cells expressing oncogenic Ras (hereafter RasV12 cells) are detected by normal neighbors and as a result are often extruded from the tissue [1–6]. RasV12 cells are eliminated apically, suggesting that extrusion may be a tumor-suppressive process. Extrusion depends on E-cadherin-based cell-cell adhesions and signaling to the actin-myosin cytoskeleton [2, 6]. However, the signals underlying detection of the RasV12 cell and triggering extrusion are poorly understood. Here we identify differential EphA2 signaling as the mechanism by which RasV12 cells are detected in epithelial cell sheets. Cell-cell interactions between normal cells and RasV12 cells trigger ephrin-A-EphA2 signaling, which induces a cell repulsion response in RasV12 cells. Concomitantly, RasV12 cell contractility increases in an EphA2-dependent manner. Together, these responses drive the separation of RasV12 cells from normal cells. In the absence of ephrin-A-EphA2 signals, RasV12 cells integrate with normal cells and adopt a pro-invasive morphology. We also show that *Drosophila* Eph (DEph) is detected in segregating clones of RasV12 cells and is functionally required to drive segregation of RasV12 cells in vivo, suggesting that our in vitro findings are conserved in evolution. We propose that expression of RasV12 in single or small clusters of cells within a healthy epithelium creates ectopic EphA2 boundaries, which drive the segregation and elimination of the transformed cell from the tissue. Thus, deregulation of Eph/ephrin would allow RasV12 cells to go undetected and expand within an epithelium.

## RESULTS AND DISCUSSION

Based on our previous findings [2], we hypothesized that extrusion of RasV12 cells is triggered by cell-cell signals at the RasV12-normal interface. To identify these signals, we designed the cell confrontation assay in order to amplify the interface

between RasV12 and normal epithelial cells, and we used Madin-Darby canine kidney (MDCK) epithelial cell culture systems, expressing GFP-tagged, constitutively active, oncogenic Ras (RasV12) in a tetracycline/doxycycline-inducible manner [2].

Normal or GFP-RasV12 cells were seeded into one of two compartments of a cell culture insert separated by a fixed gap (Figure S1A), similar to as in [7]. After removing the culture insert, cells migrated to close the gap; opposing cells collided and cell-cell interaction occurred between marginal cells. Live-cell imaging experiments revealed that, upon collision with normal cells, marginal GFP-RasV12 cells collapsed (Figure S1B) and were repulsed backward, while normal cells continued to migrate forward (Figures 1A and 1B, R:N TetON; Movie S1). At 21–30 hr post-collision, RasV12 cells had tightly packed and separated from normal cells by a distinct and visible border (Figure 1A). These phenomena only occurred when GFP-RasV12 was induced in one population of cells (Figure 1B, R:N TetOFF). In contrast, when two opposing sheets of GFP-RasV12 cells collided, both populations stopped migrating (Figure 1B, R:R TetON; Movie S2) and fused to form a monolayer (Figure 1A). In the absence of cells in the second compartment, GFP-RasV12 cells continued to migrate forward into free space (Figure 1B, R:No cells). Single-cell tracking analyses confirmed that, upon collision with normal cells, RasV12 cells (either at the margin or further behind the leading edge) were repulsed backward with the same direction (Figure S1C; Movie S3). In contrast, when RasV12 cells collided with RasV12 cells, cell migration lacked directionality (Figure S1C; Movie S3). Thus, upon collision with normal cells, RasV12 cells display cell repulsion, are triggered to migrate backward, and avoid intermingling with normal cells.

Following collision with normal cells, RasV12 cells rapidly adopted a contractile morphology. We measured changes in RasV12 cell area as a readout for cell contractility, and we found that the RasV12 cell area significantly decreased following collision with normal cells, but not with RasV12 cells (Figure 1C). This decrease was observed in marginal RasV12 cells (row 1) and in RasV12 cells positioned further behind the collision interface (+11; Figure S1D). Hence, as leading RasV12 cells are repulsed, RasV12 cells behind the margin become compressed. In contrast, RasV12 cells colliding with RasV12 cells maintained a constant cell area (Figure S1D).

Consistent with our previous findings [2], we observed that F-actin accumulated specifically at cell-cell contacts between RasV12 cells that had collided with normal cells (Figure 1D).

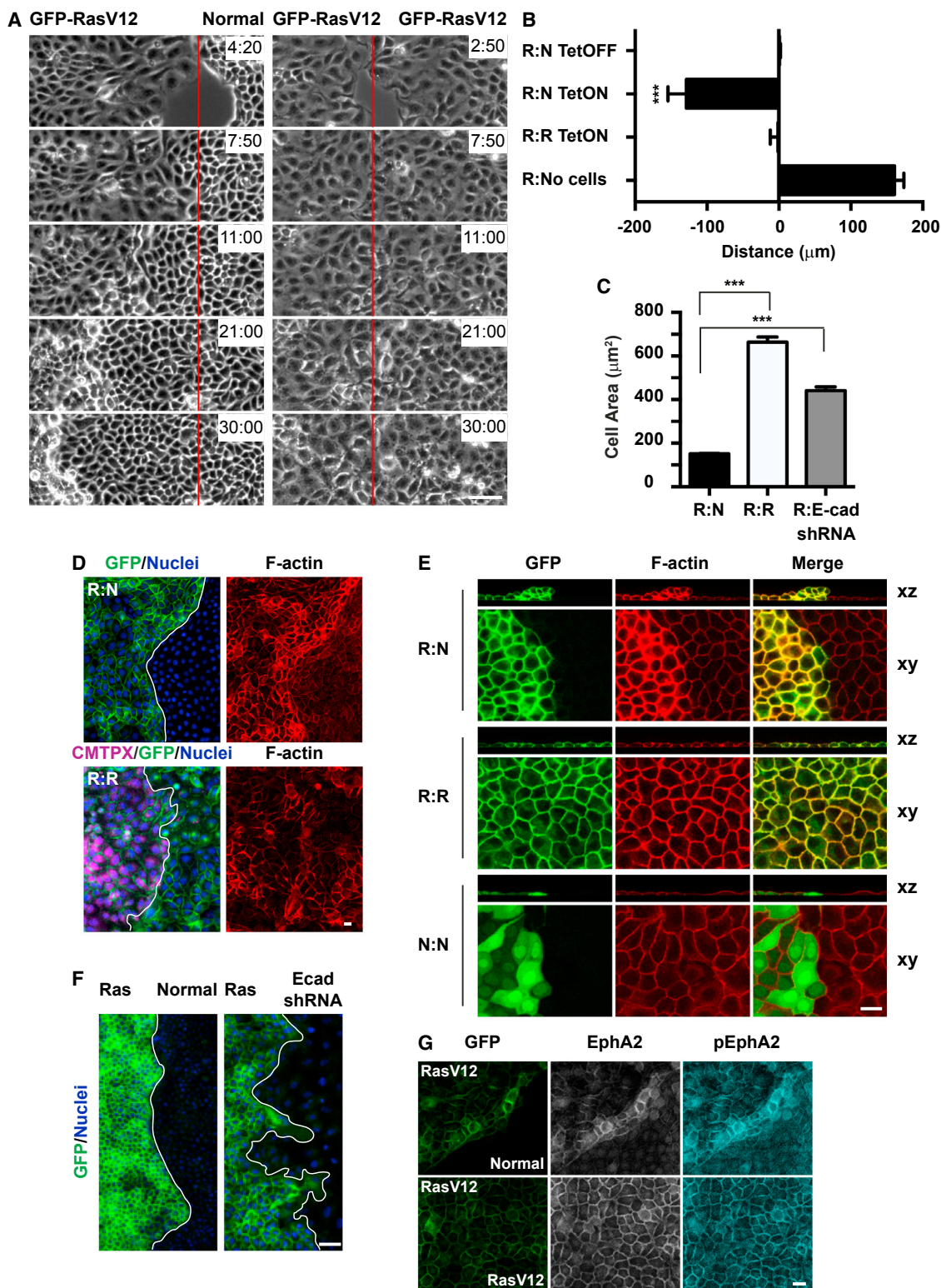


**Figure 1. Direct Cell-Cell Interaction between Epithelial Cell Sheets in a New Cell Confrontation Assay Demonstrates that Normal Cells Trigger Repulsion of RasV12 Cells**

(A) Images extracted from a representative time-lapse cell confrontation experiment showing sheets of MDCK-pTR-GFP-RasV12 cells colliding with either normal MDCK cells (left panels) or with MDCK-pTR-GFP-RasV12 cells (right panels). Elapsed time is indicated as hr:min. Red line indicates point of collision.

(legend continued on next page)

Moreover, neighboring RasV12 cells, positioned behind the collision interface and not in direct contact with normal cells, also accumulated F-actin at cell-cell contacts over time (Figures 1E, S1E, S1F, and S1I). The inhibition of myosin-II or Src family kinase (SFK) pathways reduced RasV12 contractility (Figure S1G). The inhibition of SFK, but not myosin-II, significantly decreased RasV12 cell repulsion (Figure S1H). Indeed, collision with normal cells triggered RasV12 cells to actively migrate backward, independent of myosin-II activity (Movie S4), similar to as in [8]. However, phosphorylated myosin light chain (pMLC) was detected at higher levels specifically in RasV12 cells that had collided with normal cells (Figure S1I). Although we cannot rule out that migrating normal cells also compress RasV12 cells via processes that are myosin-II independent, our findings indicate a role for myosin-II activity in RasV12 cell repulsion.

Finally, cell repulsion did not occur when RasV12 cells collided with E-cadherin-depleted cells (distance = 0  $\mu\text{m}$ ,  $n = 2$ ). Here RasV12 cell area was more comparable to that of RasV12 cells in a monolayer (Figure 1C). Moreover, RasV12 cells and E-cadherin-depleted cells separated via an irregular interface (Figure 1F). Thus, upon collision with normal cells, RasV12 cells contract and separate via a process that is dependent on E-cadherin-based cell-cell adhesion. Crucially, these experiments demonstrate that similar phenomena occur in RasV12 cells at the single-cell [2] and multicellular levels following interactions with normal cells and that a dependence on specific signaling proteins is required in both contexts.

Eph-ephrin signaling regulates cell repulsion and cell segregation, processes that prevent cell mixing and drive boundary formation during tissue development and maintenance [9]. Similar to previous reports [10, 11], we found that RasV12 cells expressed EphA2 mRNA (Figure S2A) and protein (Figure S2B) at elevated levels compared to normal cells. Expression of EphA2 protein was MEK-ERK dependent (Figure S2B). MEK-ERK signaling also was required to drive RasV12 cell extrusion [2], changes in cell area (Figure S1G), and cell repulsion (Figure S1H). Therefore, we tested whether Eph-ephrins were necessary to drive RasV12 cell repulsion.

We first performed cell confrontation assays in the presence of soluble, recombinant ephrin-Fc ligands. We reasoned that

soluble ligands would interfere with endogenous Eph-ephrin signaling, similar to as in [12–14]. Repulsion of RasV12 cells from normal cells was significantly inhibited in the presence of ephrin-A1-Fc and ephrin-A4-Fc (Figure S2C), whereas the addition of ephrin-B ligands had no effect (Figure S2C). The addition of ephrin-A1/ephrin-A4 also significantly reduced RasV12 cell contractility (Figure S2D), and it promoted cell intermingling at RasV12-normal cell interfaces (Figure S2E). The inhibitory effects of long-term treatment with ephrin-A ligands may be due to EphA2 downregulation from the cell surface ([15]; data not shown). Together, these results suggest a requirement of EphA family members in RasV12 cell responses following interaction with normal cells. Both normal and RasV12 cell lines also expressed EphA1, ephrin-A1, and ephrin-A4 at similar mRNA levels (Figure S2A). Given that EphA2 is a transcriptional target of Ras-MAPK signaling [10], we focused on the functional role of EphA2 in RasV12-normal cell-cell interaction.

In general, binding of ephrin ligand triggers Eph receptor clustering and activation by phosphorylation on conserved tyrosine residues [16, 17]. We detected elevated levels of phosphorylated EphA2 (Y594) in clusters of RasV12 cells surrounded by normal cells (Figure S3A) and in RasV12 cells that had immediately collided with, and been repulsed by, normal cells (Figure 1G). The intensity of phosphorylated EphA2 was significantly higher at the RasV12-normal interface (Figure S3B), demonstrating that activation of EphA2 is specifically occurring upon cell-cell interaction. Phosphorylated EphA2 also was detected at significantly higher levels at cell-cell contacts between RasV12 cells within a cluster (Figures S3B and S3F).

To test the functional role of EphA2, we established two GFP-RasV12 cell lines that constitutively expressed independent small hairpin RNA (shRNA) constructs targeting EphA2 (shRNA-1 or -2) as well as a scramble control (Figure S3C). When cultured with normal cells at 1:100 ratios, EphA2-depleted RasV12 cells no longer clustered but appeared flat and spread (Figure 2A). As expected, we did not detect elevated levels of phosphorylated EphA2 in EphA2-depleted cells (Figure 2A). To quantify the change in cell morphology, we measured the distance between the center of nuclei of neighboring cells in direct contact (inter-nuclear distance [IND]; Figure 2B). When

(B) Quantification of distance ( $\mu\text{m}$ ) traveled by marginal RasV12 cells in cell confrontation assays. Migration distances were scored following collision of cells until the end of the experiment (42 hr). Data indicate mean  $\pm$  SD from three independent experiments (\*\*\*)  $p < 0.001$  for R:N TetON versus all other conditions). Error bars show SD.

(C) Quantification of GFP-RasV12 cell area ( $\mu\text{m}^2$ ) in cell confrontation assays with normal cells (R:N, black bar;  $n = 182$  cells), with GFP-RasV12 cells (R:R, white bar;  $n = 303$  cells), or E-cadherin-depleted cells (R:E-cadherin shRNA, gray bar;  $n = 232$  cells). Data represent mean  $\pm$  SEM from three independent experiments (\*\*\*)  $p < 0.001$ . Error bars show SEM.

(D) Confocal images of confrontation assays. Upper panels: GFP-RasV12 cell sheets confront normal MDCK monolayers (R:N). Lower panels: GFP-RasV12 cell sheets confront GFP-RasV12 cells (R:R). Cells were fixed 40 hr after the addition of doxycycline ( $\sim 16$ – $18$  hr post-collision) and stained with phalloidin (red) and Hoechst (blue). One population of RasV12 cells was prestained with cell tracker dye (CMTPX, magenta) to identify the boundary between the two populations of cells following collision. White line in (D) and (F) depicts border between two populations of cells following collision.

(E) Confocal images of cell confrontation assays. Upper panels: GFP-RasV12 cell sheets confront normal MDCK monolayers (R:N). Middle panels: GFP-RasV12 cells confront GFP-RasV12 cells (R:R). Lower panels: normal GFP-labeled cells confront non-labeled normal MDCK cells (N:N). Cells were fixed 48–55 hr after the addition of doxycycline ( $\sim 24$ – $31$  hr post-collision) and stained with phalloidin (red).

(F) Confocal images of GFP-RasV12 cells confronting normal MDCK cells (left panel) or MDCK cells expressing E-cadherin shRNA (right panel). Cells were fixed 48 hr after the addition of tetracycline ( $\sim 22$ – $24$  hr post collision) and stained with Hoechst (blue).

(G) Confocal images of cell confrontation assays of GFP-RasV12 cell sheets colliding with normal (non-labeled) monolayers (top panels) and GFP-RasV12 cell sheets colliding with GFP-RasV12 cells (lower panels). Cells were fixed 30 hr after the addition of doxycycline ( $\sim 6$ – $8$  hr post collision) and stained with anti-EphA2 (gray) and anti-phospho-EphA2 (pEphA2, Y594; cyan) antibodies.

Scale bar, 20  $\mu\text{m}$  (A and D–G). See also Figure S1 and Movies S1, S2, S3, and S4.

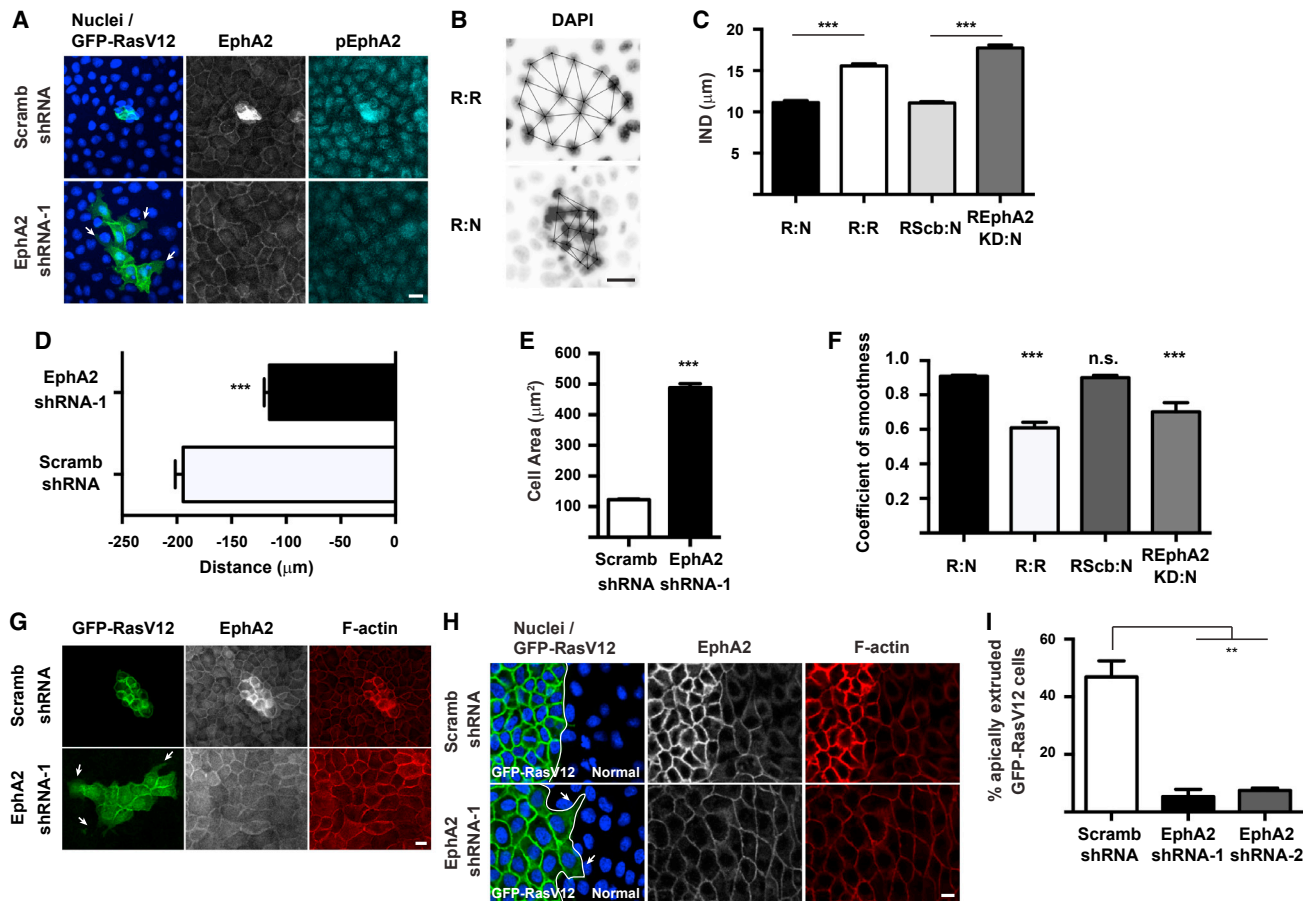


**Figure 2. GFP-RasV12 Cells Cluster, Stably Separate, and Extrude from Normal Epithelia in an EphA2-Dependent Manner**

(A) Confocal images of MDCK-pTR-GFP-RasV12 cells constitutively expressing either scramble shRNA (top panels) or EphA2 shRNA-1 (lower panels) mixed with normal MDCK cells at 1:100 ratios. Cells were fixed 48 hr after the addition of doxycycline and stained with anti-EphA2 (gray) or anti-phospho-EphA2 (pEphA2, Y594; cyan) antibodies and Hoechst (blue).

(B) Representative images illustrating quantification of inter-nuclear distance (IND) data using point-picker/Voronoi scripts. Nuclei were stained with Hoechst (DAPI). Images were inverted to grayscale using Fiji to ease visualization. Upper panel: RasV12 cells in RasV12 cell monolayers (R:R) are shown. Lower panel: RasV12 cells were mixed with normal cells at 1:100 ratios (R:N).

(C) Quantification of IND ( $\mu\text{m}$ ) between neighboring GFP-RasV12 cells in single or 1:100 co-culture assays is shown. R:N, GFP-RasV12 cells mixed with normal MDCK cells at 1:100 ratios (black bar,  $n = 148$  measurements); R:R, GFP-RasV12 cells alone (white bar,  $n = 293$  measurements); RScb:N, GFP-RasV12 cells constitutively expressing scramble shRNA mixed with normal MDCK cells at 1:100 ratios (light gray bar,  $n = 192$  measurements); REphA2 KD:N, GFP-RasV12 cells constitutively expressing EphA2 shRNA-1 mixed with normal MDCK cells at 1:100 ratios (dark gray bar,  $n = 230$  measurements). Data represent mean  $\pm$  SEM from three independent experiments (\*\* $p < 0.001$ ). Error bars show SEM.

(D) Quantification of distance ( $\mu\text{m}$ ) traveled by leading edge of GFP-RasV12 cells constitutively expressing either scramble shRNA (white bar) or EphA2 shRNA-1 (black bar) following collision with normal cells (not depicted) until the end of the experiment (42 hr). Data indicate mean  $\pm$  SEM from three independent experiments (\*\* $p < 0.001$ ). Error bars show SEM.

(E) Quantification of GFP-RasV12 cell area ( $\mu\text{m}^2$ ) in cell confrontation assays with normal cells. White bar, MDCK-pTR-GFP-RasV12 cells constitutively expressing scramble shRNA ( $n = 457$  cells); black bar, MDCK-pTR-GFP-RasV12 cells constitutively expressing EphA2 shRNA-1 ( $n = 296$  cells). Data represent mean  $\pm$  SEM from three independent experiments (\*\* $p < 0.001$ ). Error bars show SEM.

(F) Quantification of coefficient of boundary smoothness separating two populations of cells following collision in cell confrontations assays. R:N, GFP-RasV12 cells colliding with normal MDCK cells (black bar,  $n = 55$  measurements); R:R, GFP-RasV12 cells colliding with GFP-RasV12 cells (white bar,  $n = 14$  measurements); RScb:N, GFP-RasV12 cells constitutively expressing scramble shRNA colliding with normal MDCK cells (dark gray bar,  $n = 9$  measurements); REphA2 KD:N, GFP-RasV12 cells constitutively expressing EphA2 shRNA-1 mixed with normal MDCK cells (light gray bar,  $n = 10$  measurements). Data represent mean  $\pm$  SEM from at least three independent experiments (\*\* $p < 0.001$  for R:N versus R:R or REphA2 KD:N; R:N versus RScb:N is not significant [n.s.]). Error bars show SEM.

(G) Confocal images of MDCK-pTR-GFP-RasV12 cells constitutively expressing either scramble shRNA (upper panels) or EphA2 shRNA-1 (lower panels) mixed with normal MDCK cells at 1:100 ratios. Cells were fixed 48 hr after the addition of doxycycline and stained with anti-EphA2 antibody (gray) or phalloidin (red).

(H) Confocal images of cell confrontation assays. MDCK-pTR-GFP-RasV12 cell sheets expressing either scramble shRNA (top panels) or EphA2 shRNA-1 (lower panels) confront normal (non-labeled) MDCK monolayers. Cells were fixed 30 hr after the addition of doxycycline (~6–8 hr post-collision) and stained with anti-EphA2 antibodies (gray), phalloidin (red), and Hoechst (blue). White line depicts border between two populations of cells following collision.

(legend continued on next page)

surrounded by normal cells, RasV12 cells depleted of EphA2 had a significantly higher IND compared to RasV12 cells expressing scramble shRNA or parental RasV12 cells (Figure 2C), and this was more comparable to the IND value of RasV12 cells in a monolayer (Figure 2C).

In confrontation assays with normal cells, RasV12 cells depleted of EphA2 were repulsed less efficiently (Figure 2D), and they did not decrease in cell area (Figure 2E), independent of their distance to the collision margin (Figure S1D). This demonstrates that EphA2 is functionally required to induce the contraction of RasV12 cells that are both in direct contact with normal cells and further behind the collision interface. Moreover, quantification of the linearity of the border between cells ([18]; Figure 2F) indicated that depletion of EphA2 in RasV12 cells promotes local intermingling of RasV12 cells and normal cells at the cell-cell interface. Interestingly, RasV12 cells depleted of EphA2 formed large basal protrusions at the interface with normal cells (Figures 2A, 2G, and 2H), indicative of a pro-invasive morphology, also reported in [2]. F-actin did not accumulate at cell-cell contacts between RasV12 cells depleted of EphA2, either when present in normal monolayers at 1:100 ratios (Figure 2G) or following collision in confrontation assays (Figures 2H and S1E, bottom panels). Using established assays [1–5], we found that RasV12 cells depleted of EphA2 were apically extruded at a significantly lower frequency than controls (Figure 2I). Together, our data demonstrate that EphA2 expressed on RasV12 cells is activated by direct cell-cell interaction with normal cells, to induce repulsion and contraction of RasV12 cells, and it promotes the separation of RasV12 and normal cells. Moreover, EphA2 is required to induce the contraction and clustering of juxtaposed RasV12 cells that are not in direct contact with normal cells.

As signaling via SFK and myosin-II are required for RasV12 cell contractility (Figure S1G) and extrusion [2], we asked whether these signals act downstream of EphA2 in RasV12 cells. Phosphorylated (Y416) active Src was detected at elevated levels specifically in RasV12 cells surrounded by normal cells, but it was absent in RasV12 cells depleted of EphA2 (Figures S3D and S3F). In confrontation assays with normal cells, the level of pMLC was reduced in RasV12 cells depleted of EphA2 (Figure S3G). Together these data suggest that SFK and myosin-II are activated downstream of EphA2 in RasV12 cells following interaction with normal cells.

We next explored the requirement of ephrin-A ligands for RasV12 cell repulsion. Since normal cells express ephrin-A1 and -A4 ([11]; Figure S2A), we focused on examining the role of these specific ligands, first by using the cell confrontation assay. We used preclustered ephrin-A1-Fc/-A4-Fc (or Fc alone) to coat one compartment of the cell confrontation assay, and we seeded RasV12 or normal cells in the other compartment in a modified stripe assay [19]. Preclustered recombinant ephrin-Fc proteins can induce Eph receptor clustering and activate signaling [20]. We found that both RasV12 and normal cells migrated over Fc

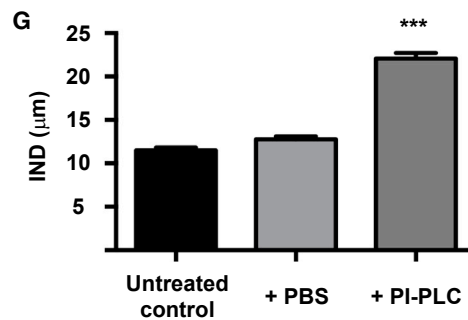
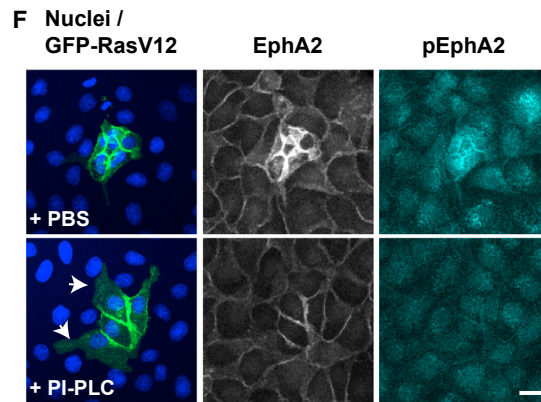
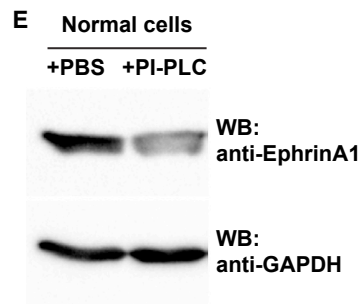
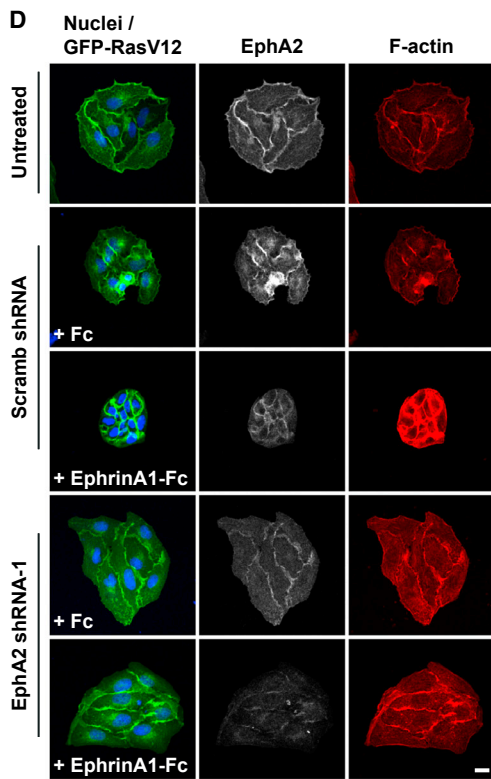
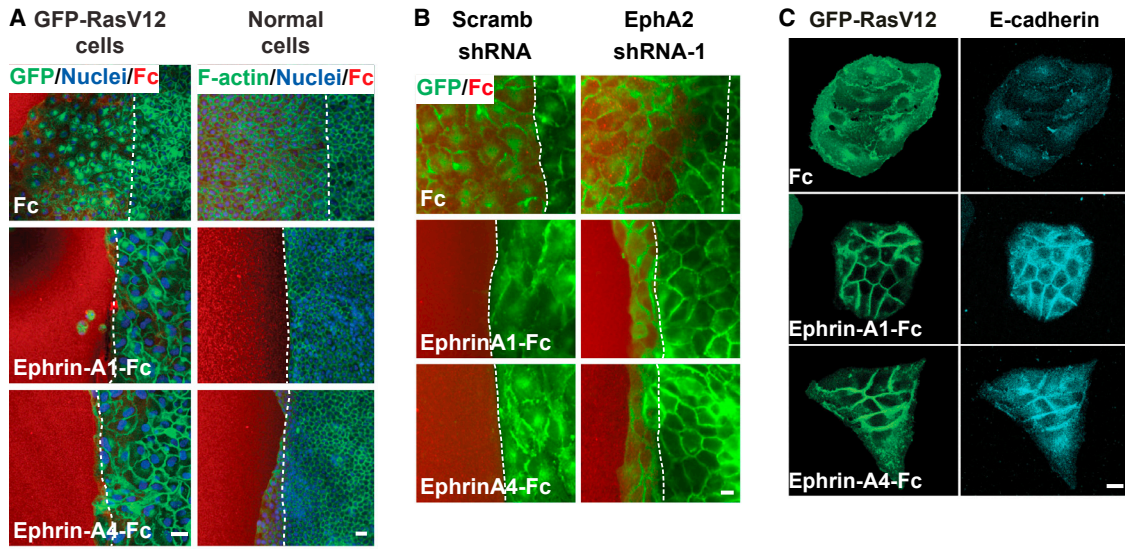
proteins (Figure 3A), but they failed to migrate over ephrin-A1-Fc ligands (Figure 3A), indicating that both cell populations are contact inhibited by ephrin-A1 ligands. RasV12 cells, and to a lesser extent the normal cells, also were contact inhibited by ephrin-A4 ligands (Figure 3A). These observations were consistent with the fact that both normal and RasV12 cells express EphA2 and EphA1 receptors, which specifically bind ephrin-A1 and/or -A4 ligands [21]. RasV12 cells depleted of EphA2 migrated (albeit weakly, most likely due to residual levels of functional EphA2 expressed on these cells; see Figure S3C) over stripes of ephrin-A1-Fc or -A4-Fc (Figure 3B), suggesting that efficient contact inhibition requires EphA2.

We predicted that, upon interaction with ephrin-A ligands, RasV12 cells also are triggered to cluster. To test this, we first seeded GFP-RasV12 cells sparsely (and in the presence of tetracycline/doxycycline) in order to promote cell scattering ([22]; Figure 3D, top panels), before treating the cells with preclustered Fc proteins. Stimulation with ephrin-A-Fc ligands induced RasV12 cells to decrease in cell area, tightly cluster, and increase E-cadherin-based cell-cell adhesion between cells (Figure 3C). Cells treated with Fc protein appeared similar to untreated cells (compare Figures 3C and 3D). Consistently, RasV12 cells expressing EphA2 shRNA (and not scramble shRNA) did not alter cell morphology or cell-cell adhesion following stimulation with ephrin-A-Fc proteins (Figure 3D).

Next, we tested whether ephrin-A ligands endogenously expressed on normal cells activate EphA2 expressed on RasV12 cells. We first treated normal cells with the enzyme phosphatidylinositol-specific phospholipase C (PI-PLC) to remove GPI-linked ephrin-A ligands [23], before mixing with RasV12 cells at 1:100 ratios. Treatment with PI-PLC significantly removed endogenous ephrin-A1 from normal cells (>80%), which remained depleted up to 24 hr after treatment (Figure 3E). The level of phosphorylated EphA2 (Y594) was markedly reduced in RasV12 cells when surrounded by PI-PLC-treated normal cells compared to RasV12 cells surrounded by PBS-treated cells (Figure 3F). RasV12 cells failed to tightly cluster in the presence of PI-PLC-treated normal cells (Figure 3G). Notably, RasV12 cells in direct contact with PI-PLC-treated normal cells formed large basal protrusions (Figure 3F), reminiscent of RasV12 cells depleted of EphA2 (Figure 2A). Taken together, our data show that ephrin-A ligands (artificially clustered or membrane bound) activate the EphA2 receptor expressed on RasV12 cells and this triggers RasV12 cells to contract and cluster with increased intercellular adhesion.

Both RasV12 and normal MDCK cell lines express comparable levels of ephrin-A ligand mRNA (Figure S2A), total protein (Figure S2F), and cell surface protein (Figure S2G). However, we never observed cell repulsion between neighboring RasV12 cells. We speculated that a difference in EphA2 expression levels between juxtaposed cells was sufficient to drive a repulsion/contractile response in the overexpressing cell. Overexpression of EphA2 in RasV12 cells could increase the cells responsiveness

(I) Quantification of apical extrusion of GFP-RasV12 cells constitutively expressing scramble shRNA (white bar), EphA2 shRNA-1 (black bar), or EphA2 shRNA-2 (gray bar) mixed with normal cells at 1:100 ratios and seeded on collagen I gels. Cells were fixed 24 hr after the addition of doxycycline. Data represent mean  $\pm$  SEM from three independent experiments (\*\* $p < 0.01$ ). Scale bar, 20  $\mu$ m (A, B, G, and H). See also Figures S1–S3.



(legend on next page)

to exogenous ephrin ligands, similar to as in [24, 25]. To test this, we carried out both 1:100 co-culture and cell confrontation assays using GFP-RasV12 cells and GFP-RasV12 cell lines, either expressing EphA2 shRNA (EphA2 knockdown [KD]) or scramble shRNA. Since RasV12 EphA2 KD cells expressed low levels of EphA2 protein similar to normal cells (Figure S3C), we predicted that these cells would behave like normal cells in these experiments. Using cell confrontation assays, we found that RasV12 cells separated from RasV12 EphA2 KD cells but intermingled with RasV12 cells expressing scramble shRNA (Figure 4A). RasV12 cell area significantly decreased following collision with RasV12 EphA2 KD cells (Figure 4B), and RasV12 cells clustered with a significantly lower IND when surrounded by RasV12 EphA2 KD cells (Figure 4C). Thus, a difference in EphA2 expression levels between juxtaposed cells is sufficient to induce cell repulsion and prevent the intermingling of the opposing cells. This in turn triggers contraction and clustering of the EphA2-overexpressing cell.

Cells expressing RasV12 in wing imaginal discs of *Drosophila melanogaster* also cluster [2], with increased DE-cadherin at cell-cell contacts, and they form uniform clones with smooth borders [26], suggesting that similar processes also occur in vivo. Indeed, cells co-expressing GFP and RasV12 formed round clusters with smooth borders that segregated them from the surrounding wild-type tissue (39.7%,  $n = 63$ ; Figures 4D and 4E). In contrast, clones of cells expressing GFP were irregular in shape and did not segregate (0%,  $n = 102$ ; Figures 4D and 4E). In *Drosophila*, a single Eph receptor (DEph) and ephrin ligand (Dephrin) have been identified, both of which play a role in the developing nervous system [27, 28]. DEph receptor also is required to maintain the straight shape of the anterior/posterior boundary in *Drosophila* [29].

Using purified Dephrin-Fc to probe for DEph expression, we observed a prominent increase in Fc staining within segregated RasV12 clusters, but not within clones of GFP-expressing cells (60% of segregated clones,  $n = 25$ ; Figures 4D and 4E). To

understand the functional significance of this observation, we expressed RNAi constructs to silence *DEph* in RasV12 cells (Figures S4A and S4B). Depletion of DEph in RasV12 clones reduced the formation of round, cyst-like clusters that stably separated from the surrounding wild-type cells (14%,  $n = 176$ ). Notably, within this population of RasV12 cells that appeared round and cyst-like, we detected elevated Dephrin-Fc staining (Figure S4C), suggesting incomplete KD of *DEph* in these cells. RasV12 clones expressing *DEph*-RNAi and displaying no detectable Dephrin-Fc staining formed irregularly shaped, non-contractile clusters (Figure 4F), and they were either aligned in the apico-basal axis (45%; Figure 4G) or remained attached to the basal layer (41%; Figure 4G) of the epithelium. In parallel, we induced RasV12 clones co-expressing a dominant-negative *DEph* transgene (DEph DN), which consists of an extracellular and transmembrane domain but lacks the intracellular domain, including the kinase domain. Hence, DEph DN should bind ligand but would be unable to signal [30]. Similar to the RNAi lines, we observed a significant decrease in round, cyst-like clusters of RasV12 cells co-expressing DEph DN (12%,  $n = 103$ ). Instead, the majority of RasV12 cells formed irregularly shaped, non-contractile clusters (88%,  $n = 103$ ) (Figure 4F), which aligned in the apico-basal axis of the tissue (Figure 4G). Thus, elevated levels of DEph are detected in segregating clones of RasV12 cells, and DEph is functionally required to drive the segregation of RasV12 cells from wild-type neighbors in vivo.

Epithelial cells expressing oncogenic v-Src also are extruded from normal monolayers via cell-cell interactions [3, 4]. Therefore, we asked whether EphA2 also is required for this process. We transiently expressed v-Src (or RasV12) with EphA2 dominant-negative (EphA2 DN), which lacks a functional intracellular domain [31], and we scored apical extrusion events. Both RasV12 and v-Src cells were extruded at significantly lower levels when cells co-expressed EphA2 DN (Figure S4D), suggesting that EphA2 signaling also is required to drive the elimination of v-Src-transformed cells from epithelial cell sheets.

### Figure 3. Ephrin-A Ligands Are Necessary for the EphA2-Dependent Phenotypes in GFP-RasV12 Cells

(A) Confocal images of GFP-RasV12 cells (left panels) or non-labeled, normal cells (right panels) confronting stripes of immobilized, pre-clustered Fc (top panels), ephrin-A1-Fc (middle panels), or ephrin-A4-Fc (lower panels) proteins. GFP-RasV12 cells were fixed 72 hr following the addition of tetracycline; normal cells were fixed at 96 hr. Normal cells were stained with phalloidin (green); both cell lines were stained with Hoechst (blue). Fc protein stripes were visualized using Alexa568-conjugated anti-goat antibodies (red). Dashed white line indicates edge of each Fc protein stripe.

(B) Epifluorescence images of MDCK-pTR-GFP-RasV12 cells constitutively expressing either scramble shRNA (left panels) or EphA2 shRNA-1 (right panels) confronting stripes of immobilized, pre-clustered Fc (top panels), ephrin-A1-Fc (middle panels), or ephrin-A4-Fc (lower panels) proteins. Cells were fixed 72 hr following the addition of doxycycline. Fc protein stripes were visualized using Alexa568-conjugated anti-goat antibodies (red). Dashed white line indicates edge of each Fc protein stripe.

(C) Confocal images of GFP-RasV12 cells seeded at low densities, incubated overnight with doxycycline before being treated with preclustered Fc (upper panels), ephrin-A1-Fc protein (middle panels), or ephrin-A4-Fc (lower panels) ( $10 \mu\text{g ml}^{-1}$ ) for 24 hr. Cells were fixed and stained with anti-E-cadherin antibodies (cyan).

(D) Confocal images of untreated MDCK-pTR-GFP-RasV12 cells (top panel) and MDCK-pTR-GFP-RasV12 cells constitutively expressing either scramble shRNA (middle panels) or EphA2 shRNA-1 (lower panels). All cells were seeded at low densities and incubated overnight with doxycycline before being treated with preclustered Fc or ephrin-A1-Fc protein ( $10 \mu\text{g ml}^{-1}$ ) for 24 hr. Cells were fixed and stained with anti-EphA2 antibodies (gray), phalloidin (red), and Hoechst (blue).

(E) Immunoblot analysis comparing the expression levels of endogenous ephrin-A1 protein from normal MDCK cell lines pre-treated with PBS (+ PBS) or phosphoinositide-specific phospholipase C (+ PI-PLC) for 4 hr before being switched back to standard media for a further 24 hr. Lysates were then harvested from cells and examined by western blotting using the indicated antibodies.

(F) Confocal images of normal MDCK cells pretreated with PBS (+ PBS; top panels) or phosphoinositide phospholipase C (+ PI-PLC; lower panels) for 4 hr before mixing with GFP-RasV12 cells at 100:1 ratios. Cells were fixed 24 hr after the addition of doxycycline and stained with anti-EphA2 (gray), anti-phosphorylated EphA2 (pEphA2, Y594; cyan), and Hoechst (blue).

(G) Quantification of IND ( $\mu\text{m}$ ) between neighboring GFP-RasV12 cells co-cultured with untreated normal MDCK cells (control, black bar;  $n = 109$  measurements) or normal cells pretreated with either PBS (+ PBS, gray bar;  $n = 88$  measurements) or PI-PLC (+ PI-PLC, dark gray bar;  $n = 107$  measurements). Data represent mean  $\pm$  SEM from three independent experiments (\*\* $p < 0.001$ ; control versus + PBS is n.s.)

Scale bar, 20  $\mu\text{m}$  (A–D and F).

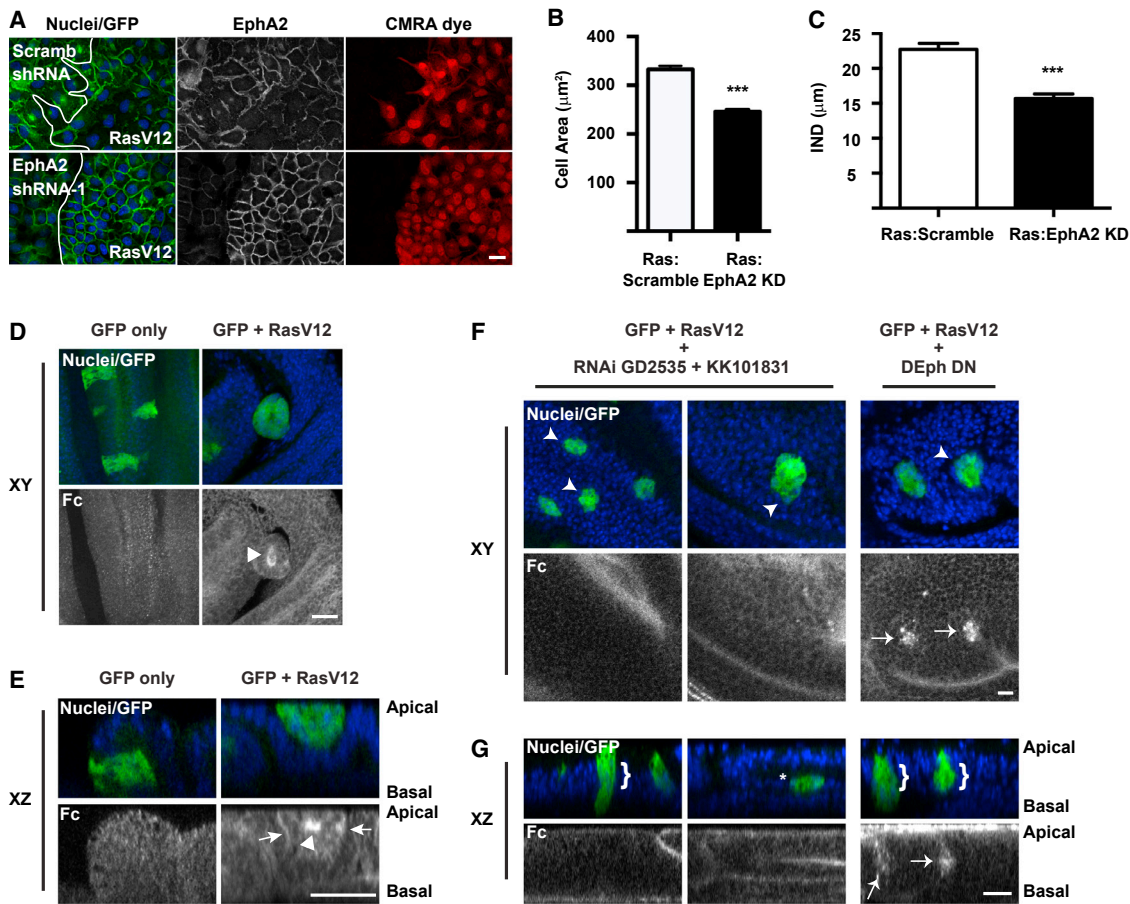


**Figure 4. Neighboring Cells Detect Differences in Eph Expression In Vitro and In Vivo, and this Triggers Segregation of the Eph-Overexpressing Cell**

(A) Confocal images of cell confrontation assays. MDCK-pTR-GFP-RasV12 cell sheets expressing either scramble shRNA (top panels) or EphA2 shRNA-1 (lower panels) confront GFP-RasV12 monolayers. GFP-RasV12 cells were prestained with CellTracker orange CMRA dye (red). Cells were fixed 48 hr after the addition of doxycycline (~22–24 hr post-collision) and stained with anti-EphA2 antibodies (gray) and Hoechst (blue). White line depicts border between two populations of cells following collision.

(B) Quantification of RasV12 cell area ( $\mu\text{m}^2$ ) in cell confrontation assays with MDCK-pTR-GFP-RasV12 cells constitutively expressing scramble shRNA (Ras:Scramble, white bar;  $n = 756$  cells) or with MDCK-pTR-GFP-RasV12 cells constitutively expressing EphA2 shRNA-1 (Ras:EphA2 KD, black bar;  $n = 1012$  cells). Data represent mean  $\pm$  SEM from three independent experiments (\*\*\*)  $p < 0.001$ .

(C) Quantification of IND ( $\mu\text{m}$ ) between neighboring RasV12 cells mixed with MDCK-pTR-GFP-RasV12 cells constitutively expressing scramble shRNA (Ras:Scramble, white bar;  $n = 80$  measurements) or with MDCK-pTR-GFP-RasV12 cells constitutively expressing EphA2 shRNA-1 (Ras:EphA2 KD, black bar;  $n = 95$  measurements) at 1:100 ratios. Data represent mean  $\pm$  SEM from three independent experiments (\*\*\*)  $p < 0.001$ .

(D and E) Confocal images of *Drosophila melanogaster* wing imaginal disc epithelia containing clones expressing GFP alone (left panels) or GFP and RasV12 (right panels). Discs were incubated with soluble Dephrin-Fc protein before being fixed and stained with anti-Fc antibody (gray) and Hoechst (blue). (D) XY images represent maximum projections of z stacks. (E) XZ images represent an orthogonal view of a z stack. White arrows indicate elevated ephrin-Fc staining at cell-cell contacts at the RasV12:Normal interface. White arrowhead indicates enhanced ephrin-Fc staining at the center of the RasV12 cell cluster.

(F and G) Confocal images of *Drosophila melanogaster* wing imaginal disc epithelia containing clones coexpressing GFP and RasV12 and either two RNAi constructs (GD2535 and KK101831) (left panels) or DEph dominant-negative (DEph DN) (right panels). Discs were incubated with soluble Dephrin-Fc protein before being fixed and stained with anti-Fc antibody (gray) and Hoechst (blue). (F) XY images represent maximum projections of z stacks. (G) XZ images represent an orthogonal view of a z stack. White arrowheads indicate irregularly shaped clones of RasV12 cells. White arrows indicate punctate Dephrin-Fc staining. White asterisk indicates a RasV12 clone in contact with the basal side of the epithelium. White brackets indicate RasV12 clones extending along the apico-basal axis of the epithelium. Scale bar, 20  $\mu\text{m}$  (A and D–G). See also [Figures S2 and S4](#).

In summary, we have found that enhanced expression of EphA2 in RasV12 cells promotes their detection by and separation from normal neighbors. Cell-cell interactions between juxtaposed cells induce EphA2 forward signaling on RasV12 cells in an ephrin-A ligand-dependent and E-cadherin-dependent manner ([Figure S4E, 1](#)). This triggers repulsion and an increase

in cell contractility of RasV12 cells in direct contact with normal cells ([Figure S4E, 2](#)). In turn, neighboring RasV12 cells that are positioned behind marginal cells and not in direct contact with normal cells are triggered to contract in an EphA2-dependent manner ([Figure S4E, 3](#)). We cannot conclusively determine whether this step is ligand dependent. It is possible

that EphA2 receptors, which are present at elevated levels on RasV12 cell membranes, become mobile [32] to form higher-order clusters in the absence of ligand, promoting autophosphorylation events [33].

Together with our previous studies, we propose that a combination of the initial repulsion signal and the concomitant contractility promotes the segregation and extrusion of RasV12 cells from normal monolayers. Our findings demonstrate that epithelial cells detect and respond to neighboring cells overexpressing Eph both in vitro and in vivo, and it is the steep difference in Eph expression levels between juxtaposed cells that is critical for this initial response. Intriguingly, within monolayers, neighboring RasV12 cells do not display cell repulsion. It is possible that inhibitory interactions in *cis* with coexpressed ephrin-A ligands [23, 25] occur on RasV12 cells, allowing a fraction of EphA2 receptors free to interact in *trans* with available ephrin-A ligands presented on neighboring normal cells, similar to as in [24, 25]. Notably, transient expression of EphA2 alone drives apical extrusion of single epithelial cells from normal monolayers at low frequencies and at protracted time points (11% extruded at 48 hr,  $n = 247$  cells), suggesting that additional signals may be required for efficient extrusion. Based on our findings, we propose that EphA2-mediated repulsion drives the segregation of RasV12 cells from normal cells, similar to mechanisms underlying cell segregation at tissue boundaries during development [34, 35]. At ectoderm-mesoderm boundaries, local Eph-ephrin signals generate local increases in myosin-II-dependent contractility, which inhibits cadherin clustering at cell-cell interfaces [36]. Our findings are distinct from S1P-dependent mechanisms of extrusion [37, 38].

Many Eph receptors are abnormally expressed during tumorigenesis, though the significance of this deregulation at the single-cell level is poorly understood. In some cancer models, ephrin-expressing normal cells compartmentalize and suppress the expansion and invasiveness of Eph receptor-overexpressing cancer cells [39, 40]. Compartmentalization of cancer cells and RasV12 cells requires E-cadherin-based cell-cell adhesions ([39]; Figure 1F). It is possible that, under pathological conditions where E-cadherin-based cell-cell adhesions are disrupted (e.g., inflammation and injury), EphA2-ephrin-A interactions between RasV12 and normal neighbors would not occur, allowing transformed cells to go undetected and spread within an epithelium. Whether segregation of abnormal cells by the normal surrounding tissue is tumor promoting or tumor suppressive will require further investigation, and the answer may provide key insights into early tumorigenesis in epithelial tissues.

#### SUPPLEMENTAL INFORMATION

Supplemental Information includes four figures, Supplemental Experimental Procedures, and four movies and can be found with this article online at <http://dx.doi.org/10.1016/j.cub.2016.09.037>.

#### AUTHOR CONTRIBUTIONS

Conceptualization, C.H.; Methodology, C.H., S.P., J.d.N., Y.Y., W.H., M.R.J., and R.M.; Investigation, C.H., S.P., J.d.N., W.H., M.R.J., and R.M.; Writing – Original Draft, C.H.; Writing – Review & Editing, C.H., J.d.N., Y.F., and S.P.; Resources (writing scripts for image analyses and *Drosophila melanogaster* experiments), J.d.N.; Supervision, C.H. and Y.F.

#### ACKNOWLEDGMENTS

We thank P.F. Copenhaver, M. Razi, and N. Mochizuki for constructs and R.E. Dearborn, the Bloomington *Drosophila* Research Center, and the Vienna *Drosophila* RNAi Center for *Drosophila* strains. C.H. would like to thank A. Lloyd, A. Lloyd lab members, and M. Marsh and B. Baum at the MRC Laboratory for Molecular Cell Biology (LMCB), University College London, for support during the early stages of this project. We thank S. Parrinello, F. Siebzenrubl, J. Sturge, and F. Afonso for critical reading of the manuscript and helpful discussions. C.H. and J.d.N. are European Cancer Stem Cell Research Institute Fellows (Cardiff University). S.P. is supported by Amser Justin Time (registered charity 1124951). Y.F. is supported by the JSPS Funding Program for Grant-in-Aid for Scientific Research on Innovative Areas and the Takeda Science Foundation. This work was supported by European Cancer Stem Cell Research Institute funding. We dedicate this work to the memory of Alan Clarke, mentor and founding director of the European Cancer Stem Cell Research Institute.

Received: December 4, 2015

Revised: July 15, 2016

Accepted: September 21, 2016

Published: November 10, 2016

#### REFERENCES

- Anton, K.A., Sinclair, J., Ohoka, A., Kajita, M., Ishikawa, S., Benz, P.M., Renne, T., Balda, M., Jorgensen, C., Matter, K., and Fujita, Y. (2014). PKA-regulated VASP phosphorylation promotes extrusion of transformed cells from the epithelium. *J. Cell Sci.* *127*, 3425–3433.
- Hogan, C., Dupré-Crochet, S., Norman, M., Kajita, M., Zimmermann, C., Pelling, A.E., Piddini, E., Baena-López, L.A., Vincent, J.P., Itoh, Y., et al. (2009). Characterization of the interface between normal and transformed epithelial cells. *Nat. Cell Biol.* *11*, 460–467.
- Kajita, M., Hogan, C., Harris, A.R., Dupre-Crochet, S., Itasaki, N., Kawakami, K., Charras, G., Tada, M., and Fujita, Y. (2010). Interaction with surrounding normal epithelial cells influences signalling pathways and behaviour of Src-transformed cells. *J. Cell Sci.* *123*, 171–180.
- Kajita, M., Sugimura, K., Ohoka, A., Burden, J., Sukanuma, H., Ikegawa, M., Shimada, T., Kitamura, T., Shindoh, M., Ishikawa, S., et al. (2014). Filamin acts as a key regulator in epithelial defence against transformed cells. *Nat. Commun.* *5*, 4428.
- Ohoka, A., Kajita, M., Ikenouchi, J., Yako, Y., Kitamoto, S., Kon, S., Ikegawa, M., Shimada, T., Ishikawa, S., and Fujita, Y. (2015). EPLIN is a crucial regulator for extrusion of RasV12-transformed cells. *J. Cell Sci.* *128*, 781–789.
- Wu, S.K., Gomez, G.A., Michael, M., Verma, S., Cox, H.L., Lefevre, J.G., Parton, R.G., Hamilton, N.A., Neufeld, Z., and Yap, A.S. (2014). Cortical F-actin stabilization generates apical-lateral patterns of junctional contractility that integrate cells into epithelia. *Nat. Cell Biol.* *16*, 167–178.
- Poujade, M., Grasland-Mongrain, E., Hertzog, A., Jouanneau, J., Chavrier, P., Ladoux, B., Buguin, A., and Silberzan, P. (2007). Collective migration of an epithelial monolayer in response to a model wound. *Proc. Natl. Acad. Sci. USA* *104*, 15988–15993.
- Matsubayashi, Y., Razzell, W., and Martin, P. (2011). 'White wave' analysis of epithelial scratch wound healing reveals how cells mobilise back from the leading edge in a myosin-II-dependent fashion. *J. Cell Sci.* *124*, 1017–1021.
- Battle, E., and Wilkinson, D.G. (2012). Molecular mechanisms of cell segregation and boundary formation in development and tumorigenesis. *Cold Spring Harb. Perspect. Biol.* *4*, a008227.
- Macrae, M., Neve, R.M., Rodriguez-Viciano, P., Haqq, C., Yeh, J., Chen, C., Gray, J.W., and McCormick, F. (2005). A conditional feedback loop regulates Ras activity through EphA2. *Cancer Cell* *8*, 111–118.
- Miura, K., Nam, J.M., Kojima, C., Mochizuki, N., and Sabe, H. (2009). EphA2 engages Git1 to suppress Arf6 activity modulating epithelial cell-cell contacts. *Mol. Biol. Cell* *20*, 1949–1959.

12. Carter, N., Nakamoto, T., Hirai, H., and Hunter, T. (2002). EphrinA1-induced cytoskeletal re-organization requires FAK and p130(cas). *Nat. Cell Biol.* *4*, 565–573.
13. Dobrzanski, P., Hunter, K., Jones-Bolin, S., Chang, H., Robinson, C., Pritchard, S., Zhao, H., and Ruggeri, B. (2004). Antiangiogenic and anti-tumor efficacy of EphA2 receptor antagonist. *Cancer Res.* *64*, 910–919.
14. Lawrenson, I.D., Wimmer-Kleikamp, S.H., Lock, P., Schoenwaelder, S.M., Down, M., Boyd, A.W., Alewood, P.F., and Lackmann, M. (2002). Ephrin-A5 induces rounding, blebbing and de-adhesion of EphA3-expressing 293T and melanoma cells by Crkl and Rho-mediated signalling. *J. Cell Sci.* *115*, 1059–1072.
15. Marston, D.J., Dickinson, S., and Nobes, C.D. (2003). Rac-dependent trans-endocytosis of ephrinBs regulates Eph-ephrin contact repulsion. *Nat. Cell Biol.* *5*, 879–888.
16. Janes, P.W., Nievergall, E., and Lackmann, M. (2012). Concepts and consequences of Eph receptor clustering. *Semin. Cell Dev. Biol.* *23*, 43–50.
17. Fang, W.B., Brantley-Sieders, D.M., Hwang, Y., Ham, A.J., and Chen, J. (2008). Identification and functional analysis of phosphorylated tyrosine residues within EphA2 receptor tyrosine kinase. *J. Biol. Chem.* *283*, 16017–16026.
18. Javaherian, S., D’Arcangelo, E., Slater, B., Zulueta-Coarasa, T., Fernandez-Gonzalez, R., and McGuigan, A.P. (2015). An in vitro model of tissue boundary formation for dissecting the contribution of different boundary forming mechanisms. *Integr. Biol. (Camb.)* *7*, 298–312.
19. Knöll, B., Weinl, C., Nordheim, A., and Bonhoeffer, F. (2007). Stripe assay to examine axonal guidance and cell migration. *Nat. Protoc.* *2*, 1216–1224.
20. Davis, S., Gale, N.W., Aldrich, T.H., Maisonpierre, P.C., Lhotak, V., Pawson, T., Goldfarb, M., and Yancopoulos, G.D. (1994). Ligands for EPH-related receptor tyrosine kinases that require membrane attachment or clustering for activity. *Science* *266*, 816–819.
21. Pasquale, E.B. (1997). The Eph family of receptors. *Curr. Opin. Cell Biol.* *9*, 608–615.
22. Potempa, S., and Ridley, A.J. (1998). Activation of both MAP kinase and phosphatidylinositol 3-kinase by Ras is required for hepatocyte growth factor/scatter factor-induced adherens junction disassembly. *Mol. Biol. Cell* *9*, 2185–2200.
23. Falivelli, G., Lisabeth, E.M., Rubio de la Torre, E., Perez-Tenorio, G., Tosato, G., Salvucci, O., and Pasquale, E.B. (2013). Attenuation of eph receptor kinase activation in cancer cells by coexpressed ephrin ligands. *PLoS ONE* *8*, e81445.
24. Eberhart, J., Swartz, M.E., Koblar, S.A., Pasquale, E.B., and Krull, C.E. (2002). EphA4 constitutes a population-specific guidance cue for motor neurons. *Dev. Biol.* *247*, 89–101.
25. Kania, A., and Jessell, T.M. (2003). Topographic motor projections in the limb imposed by LIM homeodomain protein regulation of ephrin-A:EphA interactions. *Neuron* *38*, 581–596.
26. O’Keefe, D.D., Prober, D.A., Moyle, P.S., Rickoll, W.L., and Edgar, B.A. (2007). Egfr/Ras signaling regulates DE-cadherin/Shotgun localization to control vein morphogenesis in the *Drosophila* wing. *Dev. Biol.* *311*, 25–39.
27. Scully, A.L., McKeown, M., and Thomas, J.B. (1999). Isolation and characterization of Dek, a *Drosophila* eph receptor protein tyrosine kinase. *Mol. Cell. Neurosci.* *13*, 337–347.
28. Boyle, M., Nighorn, A., and Thomas, J.B. (2006). *Drosophila* Eph receptor guides specific axon branches of mushroom body neurons. *Development* *133*, 1845–1854.
29. Umetsu, D., Dunst, S., and Dahmann, C. (2014). An RNA interference screen for genes required to shape the anteroposterior compartment boundary in *Drosophila* identifies the Eph receptor. *PLoS ONE* *9*, e114340.
30. Dearborn, R., Jr., He, Q., Kunes, S., and Dai, Y. (2002). Eph receptor tyrosine kinase-mediated formation of a topographic map in the *Drosophila* visual system. *J. Neurosci.* *22*, 1338–1349.
31. Minami, M., Koyama, T., Wakayama, Y., Fukuhara, S., and Mochizuki, N. (2011). EphrinA/EphA signal facilitates insulin-like growth factor-I-induced myogenic differentiation through suppression of the Ras/extracellular signal-regulated kinase 1/2 cascade in myoblast cell lines. *Mol. Biol. Cell* *22*, 3508–3519.
32. Salaita, K., Nair, P.M., Petit, R.S., Neve, R.M., Das, D., Gray, J.W., and Groves, J.T. (2010). Restriction of receptor movement alters cellular response: physical force sensing by EphA2. *Science* *327*, 1380–1385.
33. Wimmer-Kleikamp, S.H., Janes, P.W., Squire, A., Bastiaens, P.I., and Lackmann, M. (2004). Recruitment of Eph receptors into signaling clusters does not require ephrin contact. *J. Cell Biol.* *164*, 661–666.
34. Rohani, N., Canty, L., Luu, O., Fagotto, F., and Winklbauer, R. (2011). EphrinB/EphB signaling controls embryonic germ layer separation by contact-induced cell detachment. *PLoS Biol.* *9*, e1000597.
35. Rohani, N., Parmeggiani, A., Winklbauer, R., and Fagotto, F. (2014). Variable combinations of specific ephrin ligand/Eph receptor pairs control embryonic tissue separation. *PLoS Biol.* *12*, e1001955.
36. Fagotto, F., Rohani, N., Touret, A.S., and Li, R. (2013). A molecular base for cell sorting at embryonic boundaries: contact inhibition of cadherin adhesion by ephrin/ Eph-dependent contractility. *Dev. Cell* *27*, 72–87.
37. Slattum, G., Gu, Y., Sabbadini, R., and Rosenblatt, J. (2014). Autophagy in oncogenic K-Ras promotes basal extrusion of epithelial cells by degrading S1P. *Curr. Biol.* *24*, 19–28.
38. Yamamoto, S., Yako, Y., Fujioka, Y., Kajita, M., Kameyama, T., Kon, S., Ishikawa, S., Ohba, Y., Ohno, Y., Kihara, A., and Fujita, Y. (2016). A role of the sphingosine-1-phosphate (S1P)-S1P receptor 2 pathway in epithelial defense against cancer (EDAC). *Mol. Biol. Cell* *27*, 491–499.
39. Cortina, C., Palomo-Ponce, S., Iglesias, M., Fernández-Masip, J.L., Vivancos, A., Whissell, G., Humà, M., Peiró, N., Gallego, L., Jonkheer, S., et al. (2007). EphB-ephrin-B interactions suppress colorectal cancer progression by compartmentalizing tumor cells. *Nat. Genet.* *39*, 1376–1383.
40. Guo, H., Miao, H., Gerber, L., Singh, J., Denning, M.F., Gilliam, A.C., and Wang, B. (2006). Disruption of EphA2 receptor tyrosine kinase leads to increased susceptibility to carcinogenesis in mouse skin. *Cancer Res.* *66*, 7050–7058.